Ultrametricity in the Edwards-Anderson Model

Pierluigi Contucci,[1] Cristian Giardinà,[2] Claudio Giberti,[3] Giorgio Parisi,[4] and Cecilia Vernia[5]

[1] *Università di Bologna, Piazza di Porta S.Donato 5, 40127 Bologna, Italy*
[2] *Eurandom, P.O. Box 513 - 5600 MB Eindhoven, The Netherlands*
[3] *Università di Modena e Reggio Emilia, via G. Amendola 2 -Pad. Morselli- 42100 Reggio Emilia, Italy*
[4] *Università La Sapienza di Roma, Roma, Italy*
[5] *Università di Modena e Reggio Emilia, via Campi 213/B, 41100 Modena, Italy*

We test the property of ultrametricity for the spin glass three-dimensional Edwards-Anderson model in zero magnetic field with numerical simulations up to 20^3 spins. We find an excellent agreement with the prediction of the mean field theory. Since ultrametricity is not compatible with a trivial structure of the overlap distribution our result contradicts the droplet theory.

῾Ο ἄναξ οὗ τὸ μαντεῖόν ἐστι τὸ ἐν Δελφοῖς
οὔτε λέγει οὔτε κρύπτει ἀλλὰ σημαίνει
Heraclitus Fragment 93,
from Plutarch, On the Pythian Oracle, 404E. [1]

Ultrametricity is a widely accepted property of the mean field spin glass theory: it is a crucial ingredient in the field theoretical computations of the Sherrington-Kirkpatrick model [2, 3, 4] as well as a guiding principle for the rigorous proof of its free energy density formula [5, 6]. Its relevance in finite dimensional systems is nonetheless still an open matter, subject of intense investigations and debates in the theoretical and mathematical physics communities.

Ultrametricity states a very striking property for a physical system: essentially it says that the equilibrium configurations of a large system can be classified in a taxonomic (hierarchical) way (as animal in different taxa): configurations are grouped in states, states are grouped in families, families are grouped in superfamilies. This equilibrium ultrametricity has a correspondence in the existence of widely separated time scales in the dynamics, typically of a glassy system.

It is not clear at the present moment if ultrametricity is present in three dimensional systems; the most studied case is three dimensional spin glasses where contrasting results have been presented in the literature in the last twenty years. Part of the difficulties arise from the fact that ultrametricity should be, at the best, exact when the volume of the system goes to infinity and therefore simulations done on a limited range of volume are difficult to interpret. In this letter we study systems ranging from 4^3 to 20^3 extending of about an order of magnitude the range of volume used in previous simulations.

From the technical point of view ultrametricity implies that sampling three configurations independently with respect to their common Boltzmann-Gibbs state and averaging over the disorder, the distribution of the distances among them is supported, in the limit of very large systems, only on equilateral and isosceles triangles with no scalene triangles contribution. In a generic situation the relative weight of equilateral and isosceles triangles is arbitrary, however it is well known in *stochastically stable* systems: the *stochastic stability* property was introduced for the infinite range spin glass model in [7, 8] and later proved also for the realistic short ranged models in finite dimensions [9, 10].

The property of ultrametricity and the non-trivial structure of the overlap distribution are the characterizing features of the mean field picture and are mutually intertwined: a trivial (delta-like) overlap probability distribution, like the one predicted in the droplet theory [11], is not compatible in fact with the previous ultrametric structure because it predicts only equilateral triangles all of the same side.

In this letter we study the Edwards-Anderson model [12] for the spin glasses in the three-dimensional cubic lattice with $\pm J$ random interactions (for a numerical study in four dimensions see [13]). With a multi-spin coding and a parallel-tempering algorithm we numerically investigate the distribution of the overlaps: all the parameters used in the simulations are reported in Tab.I. We have checked the thermalization by verifying that our result would have been the same (inside our small error bar) by taking simulations a factor 4 shorter.

We find very strong indication in favor of ultrametricity which turns out to be reached at large volumes with exactly the form predicted by the mean field theory and, by consequence, a robust signal against droplet theory (for a study of dynamical ultrametricity and for the relation between statics and dynamics in spin glasses see [14, 15]). According to the literature the system has a transition T_c of 1.15 and our data are compatible with this value. The smallest temperature we used is 0.7, i.e. about $0.6T_c$: although we are relatively far from the critical temperature, we may

L	Sweeps	Nreal	n_β	T_{min}	T_{max}
4	1047552	1280	25	0.7	2.1
6	1047552	1280	25	0.7	2.1
8	1047552	1280	25	0.7	2.1
10	1047552	1280	25	0.7	2.1
12	1047552	896	25	0.7	2.1
16	2096128	1216	25	0.7	2.1
18	2096128	768	49	0.7	2.1
20	4193280	512	103	0.7	2.1

Table I: Parameters of the simulations: system size, number of sweeps, number of disorder realizations, number of temperature values allowed in the parallel tempering procedure, minimum and maximum temperature values.

still feel some effects coming from the critical region. However we notice that ultrametricity should not be valid at the critical temperature, consistent with our results, so any finding of ultrametricity at lower temperature cannot be an artefact.

From a mathematical point of view the triple $(c_{1,2}, c_{2,3}, c_{3,1})$, with $0 \leq c_{i,j} \leq 1$, representing the overlaps among three copies of the system, is called *stochastically stable and ultrametric* when, defining $\chi(c) = \int_0^c P(c')dc'$, where $P(c)$ is the probability distribution of c, its joint probability distribution function has the following structure:

$$P_3(c_{1,2}, c_{2,3}, c_{3,1}) = \frac{1}{2}P(c_{1,2})\chi(c_{1,2})\delta(c_{1,2} - c_{2,3})\delta(c_{2,3} - c_{3,1}) \tag{1}$$

$$+ \frac{1}{2}P(c_{1,2})P(c_{2,3})\theta(c_{1,2} - c_{2,3})\delta(c_{2,3} - c_{3,1})$$

$$+ \frac{1}{2}P(c_{2,3})P(c_{3,1})\theta(c_{2,3} - c_{3,1})\delta(c_{3,1} - c_{1,2})$$

$$+ \frac{1}{2}P(c_{3,1})P(c_{1,2})\theta(c_{3,1} - c_{1,2})\delta(c_{1,2} - c_{2,3}) \ .$$

Thinking of the quantities c's as 1 minus the sides of a triangle the previous formula says that only equilateral (first term on the right hand side of eq. (1)) and isosceles (last three terms of eq. (1)) triangles are allowed, the scalene triangles have zero probability. Equation (1) implies that the distribution of the three random variables $u = \min(c_{1,2}, c_{2,3}, c_{3,1})$, $v = \mathrm{med}(c_{1,2}, c_{2,3}, c_{3,1})$ and $z = \max(c_{1,2}, c_{2,3}, c_{3,1})$ is

$$\rho(u, v, z) = \frac{1}{2}\chi(u)P(u)\delta(v - u)\delta(z - v) + \frac{3}{2}P(z)P(v)\theta(z - v)\delta(v - u) \ , \tag{2}$$

and from that one deduces that the distribution of the two differences $x = v - u$, $y = z - v$ is

$$\tilde{\rho}(x, y) = \delta(x)\left[\frac{1}{4}\delta(y) + \frac{3}{2}\theta(y)\int_y^1 P(a)P(a - y)da\right] \ , \tag{3}$$

whose marginals are

$$\tilde{\rho}(x) = \delta(x) \ , \tag{4}$$

$$\tilde{\rho}(y) = \frac{1}{4}\delta(y) + \frac{3}{2}\theta(y)\int_y^1 P(a)P(a - y)da \ . \tag{5}$$

We recall that the Hamiltonian of the EA model [12] is given by

$$H_\sigma = -\sum_{|i-j|=1} J_{i,j}\sigma_i\sigma_j \tag{6}$$

with $J_{i,j} = \pm 1$ symmetrically distributed and Ising spins σ_i. Given two spin configurations σ and τ for a system of linear size L, we consider the main observables: the link-overlap

$$Q(\sigma,\tau) = (3L^3)^{-1} \sum_{|i-j|=1} \sigma_i \sigma_j \tau_i \tau_j \tag{7}$$

which is the normalized Hamiltonian covariance, and the standard overlap

$$q(\sigma,\tau) = (L^3)^{-1} \sum_i \sigma_i \tau_i \tag{8}$$

which is related to the Edwards-Anderson order parameter. For every function of two spin configurations $c(\sigma,\tau)$ (for instance Q or q) the physical model induces a probability distribution by the formula

$$\mathcal{P}_3(c_{1,2}, c_{2,3}, c_{3,1}) = \langle \delta(c_{1,2} - c(\sigma,\tau)) \delta(c_{2,3} - c(\tau,\gamma)) \delta(c_{3,1} - c(\gamma,\sigma)) \rangle \ , \tag{9}$$

where σ, τ, γ denote three different equilibrium configurations. Here and in the sequel the brackets $\langle \cdot \rangle$ will denote the average over the disorder $J_{i,j}$ of the thermal average over the Boltzmann-Gibbs distribution.

We will find very strong evidences that for large volumes the link overlap has the ultrametric structure of eq. (1). (we are in zero magnetic field and the system is invariant under a global change of all the spins). As we shall see at the end of the paper the same results are valid also for the standard overlap with the only difference that it has a symmetric distribution in the interval $[-1, 1]$ and the triangle distribution is built on it by suitable contributions of the positive and negative values, see formula (10) below.

We present firstly the results for the link overlap for two reasons: the analysis is conceptually simpler, the link overlap is more fundamental than the standard overlap and contains more interesting information, e.g. two configurations that differ by a spin inversion of a compact region of size half of the lattice, will have, in the infinite volume limit, a zero standard overlap, but a large link overlap.

The results can be described as follows. We test numerically the structure of the distribution for the two random variables $X = Q_{med} - Q_{min}$ and $Y = Q_{max} - Q_{med}$ where the Q's represent the largest, medium, and smaller value of the link-overlap among three copies of the system. The numerical data are compared to the formulas (4) and (5).

- Figure 1: We find that the variances of the two variables have a totally different behavior. The left panel contains the plot of $Var(X)/Var(Q)$ and the right panel of $Var(Y)/Var(Q)$ both as a function of $Var(Q)$. We find more convenient this parametrization with respect to the usual one using temperature because it allows to extract more information on size dependence through scaling laws: this is due to the fact that both $Var(Y)$ and $Var(Q)$ have size dependence changing with T. In particular within the temperature range that we have taken into account the quantity $Var(Q)$ decreases monotonically with the temperature. The figure clearly shows that while the variance of X is shrinking to zero the variance of Y is growing with the volume. Moreover the variance of X satisfy a scaling law with very good accuracy: $Var(X)/Var(Q)$ scales like $L^{-1.18}$ (see inset) while there is no scaling law for the second variable.

- Figure 2: The figure displays for two system sizes of $L = 12$ and $L = 20$ the data histograms for X (in black) and Y (in red) variable at $T = 0.7$. They show that $\mathcal{P}(X)$, the empirical distribution of X, is much more concentrated close to zero, while $\mathcal{P}(Y)$ is spread on a larger scale. The function $\tilde{\rho}(Y)$ provides a test of consistency with formula (5). The plot of $\tilde{\rho}(Y)$ has been obtained using the data histograms for the function of X to represent the delta function (4) and the experimental data for the distribution of Q inside the convolution. The two curves superimpose each other with an excellent agreement. We have also tested that any different numerical weight other than 1/4 and 3/4 do not yield such an agreement.

The previous results clearly show that the link overlap has an ultrametric distribution. Our next investigation is about the standard overlap for which we find that it also obeys ultrametricity. Given the three standard overlaps $q_{1,2}, q_{2,3}, q_{1,3}$ their probability measure is a priori supported on $[-1, 1]^3$. Reflection invariance ($q_{i,j} \to \alpha_i q_{i,j} \alpha_j$, with $\alpha = \pm 1$) implies that it is a sum of two orbits, one for $S = \mathrm{sign}(q_{1,2} q_{2,3} q_{1,3}) > 0$ and the other for $S < 0$. The mean field theory predicts that only non-frustrated triples ($S > 0$) contribute to the triangle distribution, namely:

$$\bar{P}_3(q_{1,2}, q_{2,3}, q_{3,1}) = \frac{1}{4} \left[P_3(q_{1,2}, q_{2,3}, q_{3,1}) \theta(q_{1,2}) \theta(q_{2,3}) \theta(q_{3,1}) + P_3(-q_{1,2}, -q_{2,3}, q_{3,1}) \theta(-q_{1,2}) \theta(-q_{2,3}) \theta(q_{3,1}) \right. \tag{10}$$

$$\left. + P_3(q_{1,2}, -q_{2,3}, -q_{3,1}) \theta(q_{1,2}) \theta(-q_{2,3}) \theta(-q_{3,1}) + P_3(-q_{1,2}, q_{2,3}, -q_{3,1}) \theta(-q_{1,2}) \theta(q_{2,3}) \theta(-q_{3,1}) \right]$$

To check the validity of the previous formula it is convenient to introduce the new random variables

$$\tilde{q}_{max} = \max(|q_{1,2}|, |q_{2,3}|, |q_{1,3}|) \tag{11}$$

$$\tilde{q}_{med} = \mathrm{med}(|q_{1,2}|, |q_{2,3}|, |q_{1,3}|) \tag{12}$$

$$\tilde{q}_{min} = \mathrm{sign}(q_{1,2}q_{2,3}q_{1,3}) \min(|q_{1,2}|, |q_{2,3}|, |q_{1,3}|) \tag{13}$$

and verify that their distribution is the (1). The numerical results are illustrated in Fig 3: the left panel shows how the normalized variance of the variable $\tilde{x} = \tilde{q}_{med} - \tilde{q}_{min}$ has a clear tendency to vanish for temperatures below the critical point. The inset displays the log-log plot of $Var(\tilde{x})/Var(|q|)$ as a function of L at the lowest available temperature $T = 0.7$. At the critical point the quantity is instead size invariant as predicted by the mean field theory. A totally different behaviour is found for the variable $\tilde{y} = \tilde{q}_{max} - \tilde{q}_{med}$ where below the critical temperature the normalized variance is increasing but still size invariant at criticality.

We have also explicitly investigated the contribution of the frustrated triples by plotting the quantity $S^{(-)} = \int_{-1}^{0} d\tilde{q}_{min} p(\tilde{q}_{min}) \tilde{q}^2_{min} / \int_{-1}^{1} d\tilde{q}_{min} p(\tilde{q}_{min}) \tilde{q}^2_{min}$: the left panel of Fig. 4 clearly shows that the distribution of $\tilde{q}_{min}$ is supported almost completely on the positive interval and that the negative values are concentrated near zero (for similar quantities and other three-replicas observables see [16]). This implies that the contribution associated to the frustrated orbit ($S < 0$) is very small at large volumes.

The equivalent behavior of link and standard overlap is indeed expected because it extends previous findings of [17, 18] where it was shown that link and standard overlaps are mutually non fluctuating for the case of Gaussian couplings. In the right panel of Fig. 4 we show for the model with $\pm J$ investigated within this work the analysis of the relative fluctuation and functional dependence of the two overlaps. It is shown the function $G(q^2) = \langle Q|q^2\rangle$, i.e. the expected value of the link-overlap for an assigned value of the standard overlap, for different system sizes at $T = 0.7$, with a fit to the infinite volume limit $g_\infty(q^2)$. The conditional variance of Q given q^2, displayed in the inset, shows a trend toward a vanishing value for infinite system sizes.

Numerical simulations, like the Delphi Oracle for Heraclitus, neither conceal or reveal the truth, but only hint at it. In this work we have investigated the property of ultrametricity in a short-range spin-glass model. We have shown that violations of ultrametricity in finite volumes have a clear tendency to vanish as the system size increases. We verified moreover that the analytical predictions of the ultrametric replica symmetry breaking ansatz are correct up to the tested sizes. Our results contradict previous finding [19] done for much smaller volumes (up to 8^3) in which lack of ultrametricity was claimed. We have shown instead strong numerical evidence that the spin glass in three dimensions fulfills the property of ultrametricity for both the link and the standard overlap distributions. A detailed account of the present investigation will appear elsewhere [20].

Acknowledgments. We thank S. Graffi, F. Guerra, E. Marinari, C. Newman, D. Stein and F. Zuliani for useful discussions. C. Giardinà and C. Vernia acknowledge GNFM-INdAM for financial support.

[1] G.S.Kirk, J.E.Raven,M.Schofield., *The Presocratic Philosophers* Cambridge University Press (1995)
[2] D. Sherrington and S. Kirkpatrick, *Phys. Rev. Lett.* **35**, 1792 (1975).
[3] M. Mezard, G. Parisi, M.A. Virasoro, *Spin Glass Theory and Beyond* World Scientific, Singapore (1987).
[4] G. Parisi, F. Ricci-Tersenghi, *J. Phys. A: Math. Gen.* **33**, 113, (2000).
[5] F. Guerra, *Comm. Math. Phys.* **233**, 1, (2003).
[6] M. Talagrand, *Annals of Math.* **163**, 221 (2006). This result is announced in *C.R.A.S.* **337**, 111, (2003).
[7] M. Aizenman, P. Contucci *J. Stat. Phys.* **92**, 765, (1998).
[8] F. Guerra, *Int. Jou. Phys. B* **10**, 1675, (1997).
[9] P. Contucci, *J. Phys. A: Math. Gen.* **36**, 10961, (2003).
[10] P. Contucci, C. Giardinà, *Jour. Stat. Phys.* to appear (2006). *math-ph/0505055*
[11] D.S. Fisher and D.A. Huse, *Phys. Rev. Lett.* **56**, 1601 (1986)
[12] S.F. Edwards and P.W. Anderson, *Jou. Phys. F.*, **5**, 965, (1975).
[13] A. Cacciuto, E. Marinari, G. Parisi *J. Phys. A: Math. Gen* **30** L263-L269 (1997)
[14] S. Franz, F. Ricci-Tersenghi *Phys. Rev. E* **61**, 1121-1124 (2000)
[15] S. Franz, M.Mezard, G.Parisi, L.Peliti *Phys. Rev. Lett.* **81**, 1758 (1998)

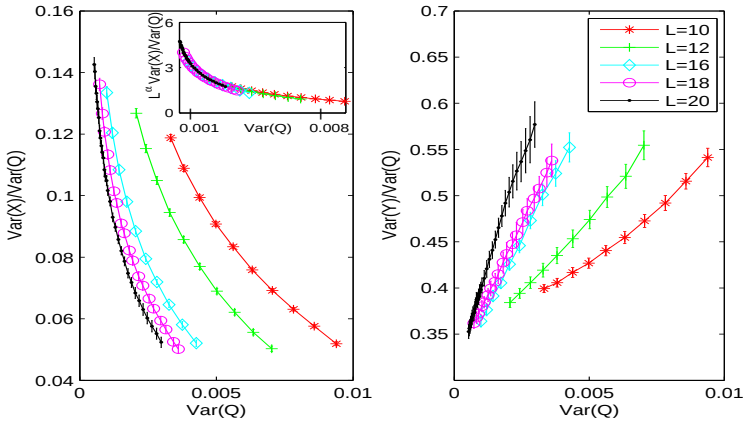

Figure 1: Normalized variances of the two random variables $X = Q_{med} - Q_{min}$ (left) and $Y = Q_{max} - Q_{med}$ (right) as a function of $Var(Q)$. The inset (at left) shows the scaling law for $\alpha = 1.18$, i.e. $L^{\alpha}Var(X)/Var(Q)$ is L-independent.

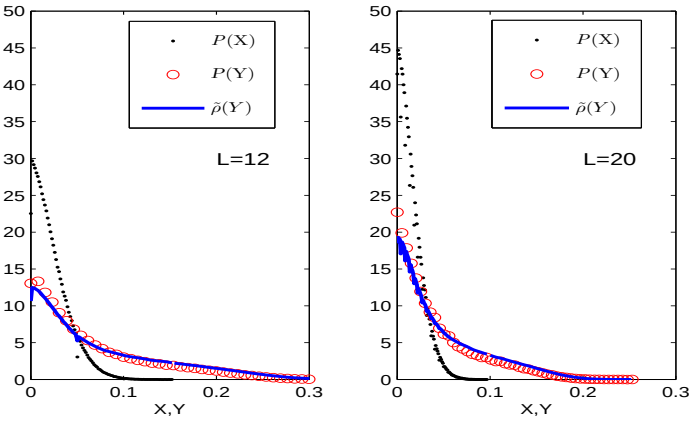

Figure 2: Empirical distributions $\mathcal{P}(X)$ and $\mathcal{P}(Y)$ for $X = Q_{med} - Q_{min}$ and $Y = Q_{max} - Q_{med}$ for the two system sizes ($L = 12$ and $L = 20$) at temperature $T = 0.7$. $\tilde{\rho}(Y)$ shows the distribution of Y computed from formula (5) using experimental data for $\mathcal{P}(Q)$ and approximating the delta function with the histogram of X

[16] D. Iñiguez, G. Parisi, J. Ruiz-Lorenzo *J. Phys. A: Math. Gen.* **29** 4337-4345 (1996)
[17] P. Contucci, C. Giardinà, C. Giberti, C. Vernia *Phys. Rev. Lett.* **96**, 217204 (2006)
[18] E. Marinari, G. Parisi *Phys. Rev. Lett.* **86**, 3887-3890 (2001)
[19] G. Hed, A. P. Young, E. Domany *Phys. Rev. Lett.* **92**, 157201 (2004)
[20] P. Contucci, C. Giardinà, C. Giberti, G. Parisi, C. Vernia, in preparation.

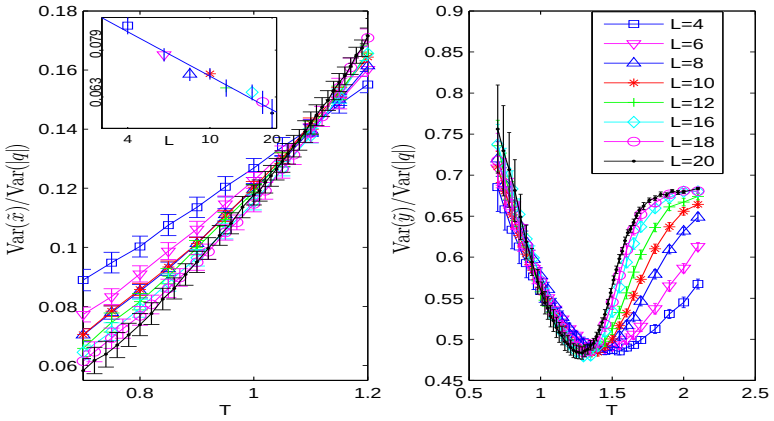

Figure 3: Normalized variances of the two random variables $\tilde{x} = \tilde{q}_{med} - \tilde{q}_{min}$ (left) and $\tilde{y} = \tilde{q}_{max} - \tilde{q}_{med}$ (right) as a function of the temperature. The inset (at left) shows the L-dependence of $Var(\tilde{x})/Var(|q|)$ at fixed temperature $T = 0.7$ on a log-log scale together with the best fit: $Var(\tilde{x})/Var(|q|) \sim aL^b$, $a = 0.12, b = -0.23$.

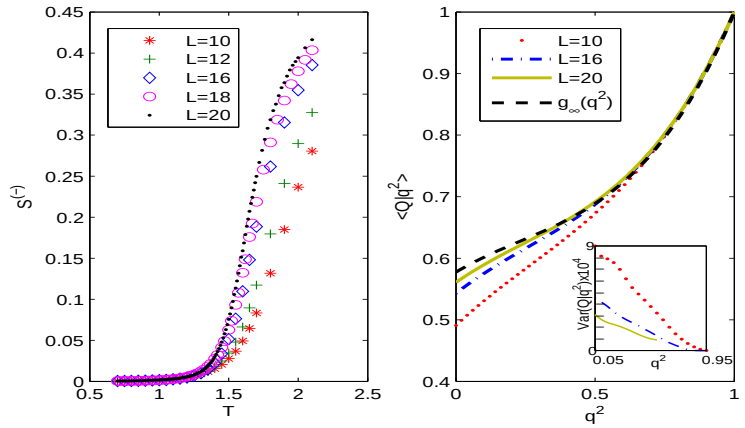

Figure 4: Left panel: the average value of $S^{(-)}$ (defined in the text) as a function of T. Right panel: Conditional expectation $\langle Q|q^2\rangle$ and conditional variance $Var(Q|q^2)$(inset) of the random variable Q given q^2, where Q is the link-overlap and q^2 is the square of the standard overlap, for different system sizes at temperature $T = 0.7$